

# On the distribution of surface extrema in several one– and two–dimensional random landscapes

F. Hivert<sup>1</sup>, S.Nechaev<sup>2,4</sup>, G.Oshanin<sup>3,\*</sup>, O.Vasilyev<sup>3,4,†</sup>

<sup>1</sup>*Institut Gaspard Monge, Université de Marne-la-Vallée 5, 77454 Marne la Vallée Cedex 2, France*

<sup>2</sup>*LPTMS, Université Paris Sud, 91405 Orsay Cedex, France*

<sup>3</sup>*LPTMC, Université Paris 6, 4 Place Jussieu, 75252 Paris, France*

<sup>4</sup>*L.D. Landau Institute for Theoretical Physics, 117334, Moscow, Russia*

(Dated: September 23, 2005)

We analyze the structure of the enveloping surface in one– and two–dimensional models of ballistic growth and calculate the corresponding probability distribution function of the number of maximal points (i.e., local “peaks”) of such a surface. Our analysis is based on two central results: (i) the proof, presented here, of the fact that uniform one–dimensional ballistic growth process in the steady state can be mapped onto “rise-and-descent” sequences in the ensemble of random permutation matrices; and (ii) the fact, established in Ref. [22], that different statistical characteristics of “rise-and-descent” sequences in random permutations can be suitably represented in terms of a certain continuous–space Hammersley-type process, which allows for a straightforward calculation of these properties. Taking advantage of these results, we find an exact solution of the one–dimensional model. Apart of the exact distribution function of the number of local peaks, we also present some explicit results for the correlation functions characterizing the enveloping surface. For surfaces emerging in two–dimensional ballistic growth, we pursue similar approach considering the ensemble of permutation matrices with long–ranged correlations. Determining exactly the first three moments of the corresponding distribution function, we restore this distribution in the scaling limit using expansion in the Edgeworth series.

## I. INTRODUCTION

Physical properties of inhomogeneous systems created by aggregation of microscopic particles are often determined by the surface structure of the aggregate and, in particular, by surface extrema. A typical example of such an extremum–influenced behavior is furnished by the phenomenon of the dielectric breakdown between two metal plates embedded in a homogeneous dielectric medium. Here, in realistic situations, the surfaces of the plates cannot be ideally flat and the “dielectric breakdown” happens between the extremal asperities (i.e., between the local maxima of the surface) at which points the electric field becomes strong enough to create a conducting channel in a dielectric medium [1].

Within the recent years much effort has been devoted to theoretical analysis of properties of surfaces obtained by aggregation of particles. Several models describing various properties of clusters grown by different deposition processes have been proposed. To name but a few, we mention the famous Kardar–Parisi–Zhang (KPZ) [2] and the Edwards–Wilkinson (EW) models [3], models of surfaces grown by Molecular Beam Epitaxy (MBE) (see, for example, Ref.[5]), Polynuclear Growth (PNG) [6, 7, 8, 9] and by Ballistic Deposition (BD) [11, 12, 13, 14], in which case particles are sequentially added to a growing surface along ballistic trajectories with random initial positions and specified direction. Finally, we mention the so-called Parallel Computing Algorithms (PCA), where the evolution of the time horizon can be thought of as that of some non-equilibrium surface, whose average rate of growth corresponds to the density of local minima in the associated stochastic surface [17].

For these models of surface growth, a number of important theoretical advancements concerning the statistics of extrema has been made. In particular, in Ref.[4] the distributions of the maximal heights of the 1D Edwards–Wilkinson and of the KPZ interfaces were determined exactly and the relation to the so-called Airy process was established. In Ref.[7] it was realized that the height distribution of the PNG surfaces coincides with the so-called Tracy–Widom distribution characterizing the Ulam process [10], which appears in the theory of random matrices near the edges of the spectrum. In Ref.[15] it has been shown that in the thermodynamic limit BD exhibits the KPZ scaling behavior. Moreover, a discrete BD model has been shown recently to be a very convenient tool for studying the non-Abelian

---

\* Also at: Max-Planck-Institut für Metallforschung, Heisenbergstr. 3, D-70569 Stuttgart, Germany, and Institut für Theoretische und Angewandte Physik, Universität Stuttgart, Pfaffenwaldring 57, D-70569 Stuttgart, Germany

† Present address: Center for Molecular Modelling, Materia Nova, University of Mons-Hainaut, Mons, Belgium

entanglement properties of braided directed random walks [16]. Finally, it has been found that in many models of ballistic growth, as well as in their continuum-space counterparts belonging to the KPZ universality class [2], the average velocity of cluster's growth is governed by the density of local minima of the enveloping surface [17].

In this work we analyze the structure of the enveloping surface emerging in one- and two-dimensional models of ballistic growth and calculate the Probability Distribution Function (PDF) of the number of maximal points (i.e., local “peaks”) of such a surface. Our analysis is based on two central concepts: (i) a proof, presented here, of the fact that a one-dimensional ballistic growth process in the steady state can be formulated exactly in terms of a “rise-and-descent” pattern in the ensemble of random permutation matrices, and (ii) such patterns can be treated in a very efficient manner using a recently proposed algorithm of a permutation-generated random walk [22].

We hasten to remark that the expected value and the variance of the number of local peaks in surfaces grown by ballistic deposition process on a one-dimensional line and on the two-dimensional honeycomb lattice were calculated for the first time by Jean Desbois in [18]. In his approach, he used a certain decoupling of a hierarchy of coupled differential equations describing evolution of the moments of higher order. This method provides correct results at least for the first two moments of the distribution function and, apparently, may be extended further for the calculation of higher moments. However, it is not a completely rigorous approach. On contrary, our approach is mathematically exact and enables us to go beyond the results obtained in [18]. In particular, we calculate an exact probability distribution function of the number of local peaks for the one-dimensional case. Apart of that, we also present some explicit results for the correlation functions characterizing the enveloping surface. For surfaces emerging in two-dimensional ballistic growth, we reduce the problem to the analysis of the ensemble of permutation matrices with long-ranged correlations. Determining exactly the first three moments of the corresponding PDF, we obtain the distribution function in the scaling limit using expansions in the Edgeworth series.

The paper is outlined as follows. In Section II we formulate our model in one dimension, introduce the notion of the so-called permutation-generated random walks (PGRW) [22], as well as interpret the statistics of “peaks”, “rises” and “descents” in random permutations of natural series in terms of certain correlation functions characterizing the PGRW. Generalization of the developed methods to the analysis of properties of surfaces emerging in two-dimensional ballistic growth is described in Section III. Finally, in Section IV we conclude with a brief summary of our results.

## II. ONE-DIMENSIONAL BALLISTIC DEPOSITION

To set up the scene, we start by formulating a standard one-dimensional ballistic deposition model (for more details, see Ref.[15]): Consider a box divided in  $N$  columns (of unit width each) enumerated by index  $i$  ( $i = 1, 2, \dots, L$ ). For simplicity, we assume the periodic boundary conditions, such that the leftmost and the rightmost columns are neighbors.

At the initial time moment  $n = 0$  the system is empty. Then, at each tick of the clock,  $n = 1, 2, \dots, N$  we deposit an elementary cell (“particle”) of unit height and width in a randomly chosen column. Suppose that the distribution on the set of columns is uniform. Define the height,  $h(i, n)$ , in the column  $i$  at time moment  $n$ . Assume now that the cells in the nearest-neighboring columns interact in such a way that they can only touch each other by corners, but never by their vertical sides. This implies that after depositing a particle to the column  $i$ , the height of this column is modified according to the following rule:

$$h(i, n + 1) = \max\{h(i - 1, n), h(i, n), h(i + 1, n)\} + 1. \quad (1)$$

If at the time moment  $n$  nothing is added to the column  $i$ , its height remains unchanged:  $h(i, n + 1) = h(i, n)$ . A set of deposited particles forms a pile as shown in Fig.1a for  $L = 6$  columns and  $N = 6$  particles. Here, for example,  $h(1, 6) = 1$ ,  $h(2, 6) = 2$ , etc.

Now, we call as the “peaks” the local maxima of the pile. More specifically, take the set  $\mathcal{H}$  of heights at some time moment  $n$ :  $\mathcal{H} = \{h(1, n), h(2, n), \dots, h(L, n)\}$ . We call the column  $i$  containing a peak at time  $n$  if the height of this column satisfies the following two-sided inequality

$$\begin{cases} h(i, n) > h(i - 1, n) \\ h(i, n) > h(i + 1, n) \end{cases} \quad (2)$$

Note that in Fig.1a there are two peaks situated in the columns  $i = 3$  and  $i = 5$ . The collection of peaks  $\mathcal{T}$  is the subset of  $\mathcal{H}$  and forms the “roof” — the set of upmost (or “removable” [24]) particles. In Fig.1a,b peaks are denoted by gray squares and other particles — by white ones.

Our goal now is the computation of the Probability Distribution Function (PDF),  $P(M, N)$ , of having  $M$  peaks in a heap comprising  $N$  particles. Moreover, we also aim to determine the “correlation function”,  $C(l)$ , defining the conditional probability that two peaks are separated by the interval  $l$  under the condition that the interval  $l$  itself is empty (i.e. does not contain peaks). As it has been noted in the Introduction, our approach borrows the ideas of Ref.[22], developed for the analysis of the so-called “Permutation Generated Random Walk”, and the proof of the fact that a one-dimensional ballistic growth process in the steady state can be formulated exactly in terms of a “rise-and-descent” pattern in the ensemble of random permutation matrices. Such a proof is outlined below.

### A. “Updating dynamics” on permutations

The dynamics of the set of peaks  $\mathcal{T}$  in the ballistic deposition shown in Fig.1b can be mapped onto the dynamics of “peaks” in the permutation matrix. We start by describing this connection on an intuitive level. To do this, let us proceed recursively. Suppose that we deposit a first particle in the column  $i_1$  of the  $L$ -column box. Next, take the row of  $L$  elements with “1” at position  $i_1$  and “0” in all other places:  $(\overbrace{0, \dots, 0}^{i_1-1}, 1, 0, \dots, 0)$ . After dropping the second particle, say, in the column  $i_2$ , take a row  $(\overbrace{0, \dots, 0}^{i_2-1}, 1, 0, \dots, 0)$  and place it over the first one creating a stock. Suppose that at some time  $n$  a new particle is added to the column which was occupied earlier, say, at time  $m$ , i.e.  $i_n = i_m$  ( $n > m$ ). It means that we have two identical rows in a stock. In this case, we remove the first of identical rows (i.e. deposited at time  $m$ ) from the stock and eliminate the empty line by pulling down all rows deposited after time  $m$ , as it is depicted in Fig.1d. After some time, the stock will comprise  $L$  rows and, according to the described procedure, will not grow anymore but will be changed only due to updating of rows (by adding the new ones and by eliminating the old ones). By construction, this stock is an  $L \times L$  permutation matrix. Connecting the nonzero elements in nearest neighboring rows by a broken line, we can straightforwardly define the “descents”, “rises” and “peaks” in the permutation matrix—see Fig.1c. The number of peaks at time  $N$  in the  $L \times L$  permutation matrix coincides then with the number of peaks in the heap after having deposited  $N$  particles in a box of  $L$  columns.

In a rigorous approach, we have to consider two dynamical systems: one on peak sets and the other on permutations. Let us call  $E_i$  the operation which corresponds to dropping a box in the column  $i$  on a peak set. That is if  $S$  is a peak set (i.e. a subset of  $\{1, \dots, L\}$  without two consecutive numbers) then

$$E_i(S) := S \cup \{i\} / \{i-1, i+1\}. \quad (3)$$

The corresponding operation  $F_i$  on permutations is defined by

$$\mu := F_i(\sigma) \quad \text{with} \quad \mu(k) := \begin{cases} \sigma(k) & \text{if } \sigma(k) < \sigma(i) \\ L & \text{if } k = i \\ \sigma(k) - 1 & \text{if } \sigma(k) > \sigma(i) \end{cases} \quad (4)$$

To proceed, we also need to define the reverse operation on permutations,  $R_k$ , which removes the upmost row and inserts it under the row  $k$ :

$$\mu := R_k(\sigma) \quad \text{with} \quad \mu(l) := \begin{cases} \sigma(l) & \text{if } \sigma(l) < k \\ k & \text{if } \sigma(l) = L \\ \sigma(l) + 1 & \text{if } L > \sigma(l) > k \end{cases} \quad (5)$$

It is clear now that  $E_i(\sigma) = \mu$  if and only if  $R_k(\mu) = \sigma$  where  $k = \sigma(i)$  is the row of the 1 in the column  $i$ .

Denote now by  $\text{Peak}(\sigma)$  the peak set of the permutation  $\sigma$ . Then, it is obvious that for all permutation  $\sigma$

$$E_i(\text{Peak}(\sigma)) = \text{Peak}(F_i(\sigma)) \quad \text{for all } i \leq L. \quad (6)$$

This simple but crucial observation allows us to translate the dynamics on permutations to the dynamics of peak sets. We will proceed in two steps: first, we will show that the limit probability measure of the dynamical system on permutations is equi-distributed and second, we will demonstrate that the image of this probability measure by the peak-set map is the limit probability measure on peak sets.

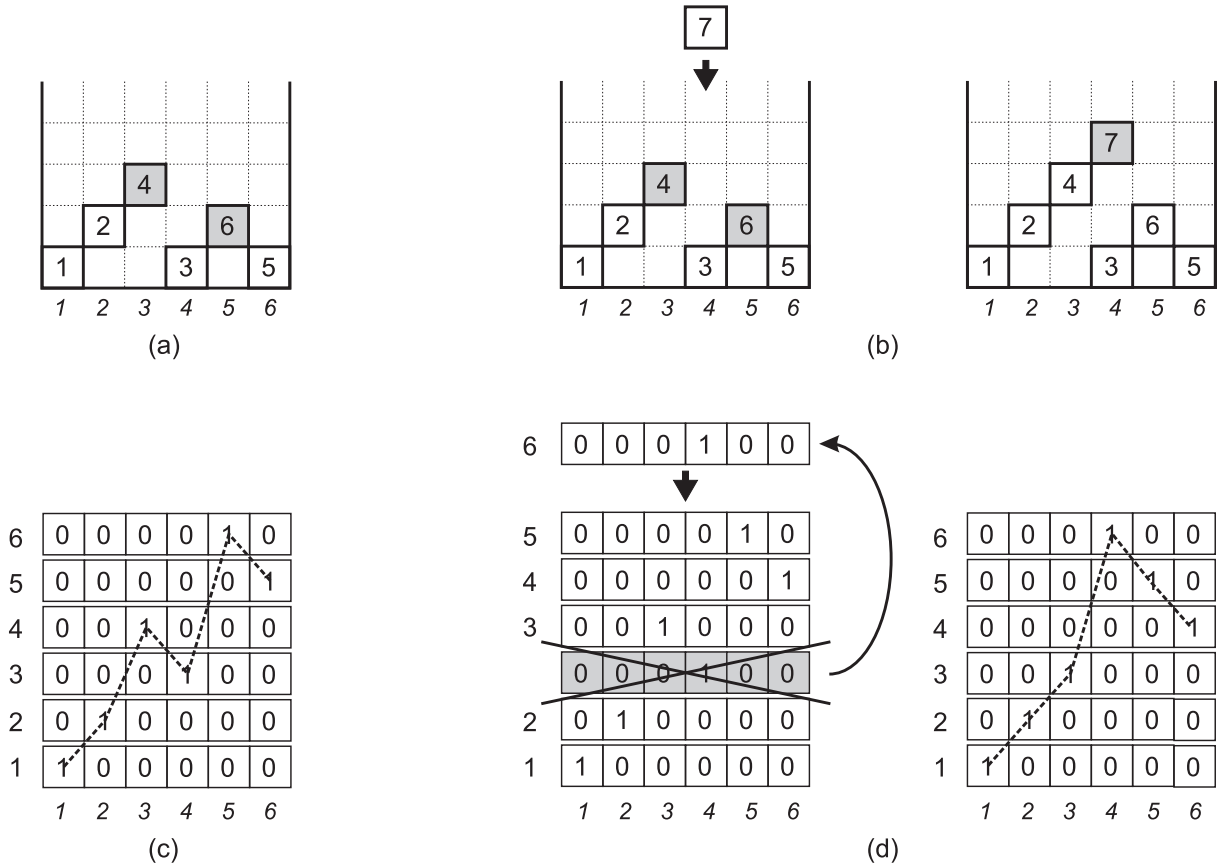


FIG. 1: Sequential growth of a heap and corresponding dynamics on permutations.

Let  $(P(\sigma))_\sigma$  be a probability measure on permutations. Then, after one uniformly random chosen step  $F_i$  the new probability  $P'(\mu)$  of a permutation  $\mu$  is

$$P'(\mu) = \frac{1}{L} \sum_{i=1}^L \sum_{\sigma} P(\sigma) \quad (7)$$

where the inner sum extends over the sets of all permutations  $\sigma$ , such that  $F_i(\sigma) = \mu$ . This is only possible if  $i$  is the column where the 1 is in the top row  $L$  in  $\mu$ , that is if  $i = \mu^{-1}(L)$ . There are exactly  $L$  such different permutations, namely  $R_k(\mu)$  for  $k = 1 \dots L$ . Consequently,  $P'(\mu)$  is simply the average of the probabilities of the  $R_k(\mu)$ :

$$P'(\mu) = \frac{1}{L} \sum_{k=1}^L P(R_k(\mu)). \quad (8)$$

Moreover, it is clear that for all pairs of permutations  $\sigma, \mu$  there is a sequence  $(i_r)_r$  of transformations which maps  $\sigma$  on  $\mu$ , that is  $\mu = \dots F_{i_3} F_{i_2} F_{i_1}(\sigma)$ . Consequently, the map  $F : P \mapsto P'$  is an irreducible Perron–Frobenius map whose maximal module eigenvalue is 1 with multiplicity 1. Thus, when the number of boxes tends to infinity, the probability converges to some limit and this limit is the unique, normalized (the sum of the coordinate is 1) eigenvector of  $F$  corresponding to the eigenvalue 1. In virtue of (8), the uniform distribution on permutations is fixed by  $F$  so that it must be the limit distribution.

Using (6), it is possible to translate our permutations language to the language of the peak sets. Recall that we call a peak set any subset of  $\{1, \dots, L\}$  without two consecutive numbers. The only needed remark is that any non empty peak set  $S$  is the peak set of a permutation. Thus the map Peak extends to a surjective map from the set of probability measure on permutations to the set of probability measures on peak sets:

$$\text{Peak} : P \mapsto \text{Peak}(P)(S) := \sum_{\sigma : \text{Peak}(\sigma)=S} P(\sigma). \quad (9)$$

Denote next  $E$  the map  $P(S) \mapsto P'(S)$  where  $P'(S)$  is the new probability measure on sets after a uniformly random step  $E_i$ . Then (6) can be written down as

$$E(\text{Peak}(P)) = \text{Peak}(F(P)), \quad (10)$$

for all probability measures on permutations  $P$ . In particular, the spectrum of  $E$  is included in the spectrum of  $F$  and moreover, the generalized eigenspaces (kernel of  $(F - \lambda I)^m$  for  $m$  large) of  $E$  are the image under  $\text{Peak}$  of the generalized eigenspaces of  $F$ . Consequently,  $E$  is a Perron–Frobenius map with maximal module eigenvalue 1 with multiplicity 1. As a consequence the limit distribution on peak sets exists and is the image by the map  $\text{Peak}$  of the limit distribution on permutations

$$P_{\text{limit}}(S) = \text{Peak}(P_{\text{limit}}(\sigma))(S) = \frac{1}{L!} \#\{\sigma \mid \text{Peak}(\sigma) = S\}. \quad (11)$$

Before we proceed further, a few comments might be in order: first, this technique is, as a matter of fact, quite general and can be applied to a much more general notion of heaps of pieces. We demonstrate it on the following example. Let  $G = (V, E)$  be a finite oriented simple graph with vertex and edge set  $V$  and  $E$  and let  $L$  be the number of vertices. Each vertex  $e \in E$  is associated with one "type" of pieces, and an arrow  $e = v \mapsto v'$  encodes the fact that when a piece of type  $v$  fall after a piece of type  $v'$ , then it is placed over it, thus they are no more pieces of type  $v'$  at the top of the pile. The notion of permutation generalizes to the notion of standard labelling of the vertex of the graph, that is assignation of distinct numbers from  $1 \dots L$  to the vertices  $v$ . Then a vertex  $v$  is called a peak of a labelling  $l$  if  $l(v) > l(v')$  for all edge  $v \mapsto v'$ . Then, the previous reasoning applies and implies that for all set  $S$  of vertices the limit probability measure  $P_{\text{limit}}(S)$  of  $S$  to be exactly the set of maximal pieces of a random heaps on the graph  $G$  is given by (11). In this regard, the limit distribution of the 2D models can also be computed using these generalized peaks. Moreover, in the case of the oriented lines the notion of peaks reduces to the notion of a descents.

Note that the combinatorics of peaks of permutations has been recently reviewed by J. Stembridge in [19] in his study of the "peak algebra". The reader has to take care of the fact that in this context a slightly different notion of a peak was used, where the extremities 1 and  $L$  were never considered as a peak. The Peak algebra of Stembridge is the natural basis  $K_S$  indexed by peak sets  $S$  and therefore can serve as support for generating series of probability of a peak set. In this regard, the generating series of the probability of each peak set has a very simple expression

$$\sum_{L=0}^{\infty} t^L \sum_{S \subset \{1 \dots L\}} P(S) K_S = \sum_{L=0}^{\infty} \frac{t^L}{L!} \#\{\sigma \mid \text{Peak}(\sigma) = S\} = \exp(K_1 t) \quad (12)$$

where  $K_1$  is the unique peak set where  $L = 1$ . Furthermore it should be noticed that in [21] a different random walk is considered on peaks and conjectured on permutations with the same limit probability measure. And finally, the result of [20] suggests that this measure should be seen as some kind of generalized Plancherel measure associated with the degenerated Hecke–Clifford algebra instead of the symmetric group.

We are now in position to determine exactly the probability that a random heap has a fixed number of peaks. From our previous analysis, it follows that such a probability is equal to the number of permutations of length  $L$  having exactly  $k$  peaks, divided by  $L!$ . Now, we recollect that if one considers permutation descents instead of peaks, the numbers  $A(n, k)$  of permutations of  $1 \dots n$  with exactly  $k$  descents are known as the Eulerian numbers, which obey the following three–site recursion

$$A(n, k) = (n - k + 1) A(n - 1, k - 1) + k A(n - 1, k) \quad (13)$$

which can be encoded by the recurrence relation of the generating series  $A_n(t) := \sum_k A(n, k) t^{k+1}$

$$A_1(t) = t, \quad A_n(t) = t(1 - t) \frac{d}{dt} A_{n-1}(t) + n t A_{n-1}(t). \quad (14)$$

The peak–Eulerian number  $W(n, t)$  have also been considered by Stembridge in [19] Remark 4.8. In our notations, his results attain the following form

$$W(n, k) = (n - 2k + 2) W(n - 1, k - 1) + 2k W(n - 1, K) \quad (15)$$

which in turn can be encoded by the recurrence relation of the generating series  $W_n(t) := \sum_k W(n, k) t^k$  (note that compared to Stembridge there is no  $t^{k+1}$  term)

$$W_1(t) = t, \quad W_n(t) = 2t(1 - t) \frac{d}{dt} W_{n-1}(t) + n t W_{n-1}(t). \quad (16)$$

Here is a table of the first value

$$\begin{aligned}
W_1(t) &= t \\
W_2(t) &= 2t \\
W_3(t) &= 2t^2 + 4t \\
W_4(t) &= 16t^2 + 8t \\
W_5(t) &= 16t^3 + 88t^2 + 16t \\
W_6(t) &= 272t^3 + 416t^2 + 32t \\
W_7(t) &= 272t^4 + 2880t^3 + 1824t^2 + 64t \\
W_8(t) &= 7936t^4 + 24576t^3 + 7680t^2 + 128t \\
W_9(t) &= 7936t^5 + 137216t^4 + 185856t^3 + 31616t^2 + 256t
\end{aligned}$$

Using derivative, this allows to find a recurrence relation for all the moments of the probability measure. For example, the expectation of the number of peaks is  $\frac{n+1}{3}$  for  $n \geq 2$ ; the variance is  $\frac{2n+2}{45}$  for  $n \geq 4$ ; the third moment is  $-\frac{2n+2}{945}$  for  $n \geq 8$ .

### B. Permutation generated random walks

In this subsection we briefly outline the basic notions concerning the so-called Permutation Generated Random Walk (PGRW) [22]. Consider some particular permutation  $\pi = \{\pi_1, \pi_2, \pi_3, \dots, \pi_{L+1}\}$  of  $L + 1$  natural numbers and rewrite it as a 2-line table:

$$\pi = \begin{pmatrix} 1 & 2 & 3 & \dots & L+1 \\ \pi_1 & \pi_2 & \pi_3 & \dots & \pi_{L+1} \end{pmatrix}.$$

Suppose that this table assigns some discrete “time” variable  $s$  ( $s = 1, 2, 3, \dots, L + 1$ , upper line in the table) to each permutation encountered in the second line and, hence allows to order this permutation.

Now, in a standard notation, we call the permutation  $\pi_s$  the “rise”, if  $\pi_s < \pi_{s+1}$ , otherwise, if  $\pi_s > \pi_{s+1}$ , we refer to it as the “descent”. Further on, if for the permutation  $\pi_s$  we have simultaneously  $\pi_{s-1} < \pi_s$  and  $\pi_s > \pi_{s+1}$ , we call it the “peak”.

Then, the Permutation Generated Random Walk is defined by the following recursive procedure:

- i) at time moment  $s = 0$  the walker stays at the origin;
- ii) at the time  $s > 0$  the walker makes step to the right if the permutation  $\pi_s$  is the rise, and makes the step to the left if the permutation  $\pi_s$  is the descent.

Note that, evidently, if the permutation  $\pi_s$  is a peak, then the walker has a right “turning point”.

Statistical properties of the PGRW were studied in Ref.[22], where the distribution of the end-to-end distance, intermediate points, the number of turns of the trajectories, as well as various correlation functions have been analyzed with respect to the uniform measure on the ensemble of random permutations.

Using the methods developed in Ref.[22], and exploiting the connection between the one-dimensional ballistic deposition process and dynamics on permutations established in the previous section, one can straightforwardly reconstruct the probability distribution  $P(M|N, L)$  of having  $M$  peaks after uniform ballistic deposition of  $N$  particles in the planar box of  $L$  columns. The generating function,  $\mathcal{Z}(k, z)$ , of the Fourier-transformed PDF  $P(2M, L)$ ,

$$\mathcal{Z}(k, z) = \sum_{n=2}^{\infty} z^n \sum_{k=-\infty}^{\infty} e^{ikM} P(2M, L), \tag{17}$$

reads (see Eq.(87) of [22])

$$\mathcal{Z}(k, z) = \frac{4}{(1 + e^{ik})^2 z} \left[ \left( \frac{1 - e^{ik}}{1 + e^{ik}} \right)^{1/2} \coth \left( (1 - e^{2ik})^{1/2} \frac{z}{2} \right) - 1 \right]^{-1} - \frac{2}{1 + e^{ik}} - z. \tag{18}$$

Note that here we have taken into account that  $\mathcal{N}$  in [22] is equal to our  $2M$ .

In the asymptotic limit  $L \gg 1$  all the integrals can be evaluated near the saddle points, giving the following Gaussian distribution for the number of peaks of the one-dimensional ballistic deposition (compare to Eq.(92) of [22]):

$$P(M, L) \sim \frac{3}{2} \sqrt{\frac{5}{\pi L}} \exp \left\{ -\frac{45(M - \frac{1}{3}L)^2}{4L} \right\}. \quad (19)$$

Computing the three first moments of the distribution (19) for  $L \gg 1$ , we get:

$$\begin{cases} \mu_1^{1D} = \sum_{M=1}^L M P(M, L) = \frac{1}{3}L, \\ \mu_2^{1D} = \left\langle (M - \langle M \rangle)^2 \right\rangle = \frac{2}{45}L, \\ \mu_3^{1D} = \left\langle (M - \langle M \rangle)^3 \right\rangle = 0. \end{cases} \quad (20)$$

Note that the first two expressions coincide with the expectation and the variance computed by J.Desbois in [18] using decoupling of the hierarchy. What concerns the third central moment  $\mu_3^{1D}$  of the distribution  $P(M, L)$ , naturally, it turns to be equal to 0 in the Gaussian limit. In what follows we proceed to show using the method of the correlation functions (see the next Section for details) that it may be calculated exactly going beyond the Gaussian approximation (i.e. for large but finite  $L$ ). As a matter of fact, the value of  $\mu_3^{1D}$  is

$$\mu_3^{1D} = \left\langle (M - \langle M \rangle)^3 \right\rangle = -\frac{2}{945}L, \quad (21)$$

i.e. it is not zero and grows linearly with the system size  $L$ .

The computation of the conditional probability,  $C(l)$ , to find the interval of length  $l$  free of peaks, is based on the correlation function technique involving the concepts of the “rise-and-descent” operators. The corresponding operator formalism is described below for the one-dimensional BD and is generalized in the Section III to the two-dimensional BD.

### C. Correlation functions of the PGRW in operator formalism

The paper [22] proposes a simple method, (based on a Hammersley-type process developed for the analysis of the longest increasing subsequence problem), of computing the statistical weights of uniformly distributed permutations for any prescribed “rise-and-descent” sequence. Following Ref.[22], consider some given “rise-and-descent” sequence  $\alpha(L+1)$  of length  $L+1$  of the form:

$$\alpha(L+1) = \{\uparrow, \uparrow, \downarrow, \dots, \uparrow\}$$

Assign next to each rise ( $\uparrow$ ) and to each descent ( $\downarrow$ ) the operators  $I_\uparrow$  and  $I_\downarrow$ , where

$$\hat{I}_\uparrow = \int_x^1 dx' \quad \text{and} \quad \hat{I}_\downarrow = \int_0^x dx'. \quad (22)$$

To each  $L$ -step trajectory we associate the characteristic polynomial  $Q(x)$  defined as the “time-ordered” product

$$Q(x, L) = \prod_{i=1}^L \hat{I}_{\alpha_i} \cdot 1, \quad (23)$$

where  $\alpha_i = \{\uparrow, \downarrow\}$  for  $i = 1, \dots, L$ . The statistical weight, i.e. the probability distribution function,  $P(\pi_{L+1})$ , of this given “rise-and-descent” sequence  $\alpha(L+1)$  in the ensemble of all equally likely permutations is then simply given by

$$P(\alpha(L+1)) = \int_0^1 Q(x, L) dx. \quad (24)$$

For example, the sequence  $\alpha(5) = \{\uparrow, \uparrow, \downarrow, \uparrow, \uparrow\}$  has the following characteristic polynomial  $Q(x)$

$$Q(x, \alpha(5)) = \hat{I}_\uparrow \hat{I}_\uparrow \hat{I}_\downarrow \hat{I}_\uparrow \hat{I}_\uparrow \cdot 1 = \int_x^1 dx_1 \int_{x_1}^1 dx_2 \int_0^{x_2} dx_3 \int_{x_3}^1 dx_4 \int_{x_4}^1 dx_5 \cdot 1 = \frac{3}{40} - \frac{x}{8} + \frac{x^3}{12} - \frac{x^4}{24} + \frac{x^5}{120},$$

and, hence, its probability is

$$P(\alpha(5)) = \int_0^1 Q(x, \alpha(5)) dx = \frac{19}{720}.$$

The origin of (22)–(24) can be easily understood by considering the following example. Suppose there are three “markers” representing the particles with the coordinates  $x_1, x_2, x_3$  ( $0 \leq \{x_1, x_2, x_3\} \leq 1$ )—see Fig.2. Markers in Fig.2 can be independently deposited in the interval  $[0, 1]$  with uniform distribution. It is obvious that the probability  $P(\uparrow\downarrow)$  for three particles to create a peak, is defined by the probability of a configuration with  $0 \leq x_1 < x_2$  and  $x_2 > x_3 \leq 1$ . Thus,

$$P(\uparrow\downarrow) = \int_0^1 dx_3 \int_{x_3}^1 dx_2 \int_0^{x_2} dx_1 = \frac{1}{3},$$

what coincides with the operator expression

$$P(\uparrow\downarrow) = \int_0^1 \hat{I}_\uparrow \hat{I}_\downarrow dx.$$

(compare to (22)–(23)).

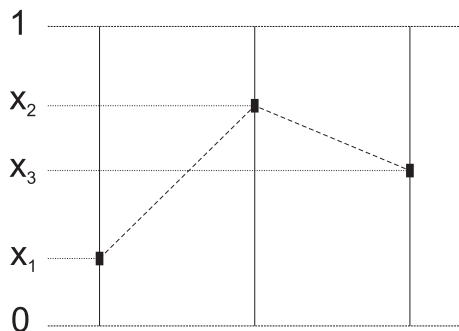


FIG. 2: Three markers creating a peak configuration.

#### D. Exact calculation of the first moments of the distribution $P(M, L)$

1. Now we apply the operator formalism for the computation of three first moments of the probability distribution function,  $P(M, L)$ , of peaks on the one-dimensional periodic lattice of size  $L$ :

$$\begin{aligned} \mu_1^{1D} &\equiv \langle M \rangle, \\ \mu_2^{1D} &\equiv \langle M^2 \rangle - \langle M \rangle^2, \\ \mu_3^{1D} &\equiv \langle M^3 \rangle - 3 \langle M \rangle \langle M^2 \rangle + 2 \langle M \rangle^3. \end{aligned} \tag{25}$$

Let us introduce

$$\Delta_i^- = \theta(x_i - x_{i-1}) \quad \text{and} \quad \Delta_i^+ = \theta(x_i - x_{i+1}), \tag{26}$$

for  $i = 1, \dots, L$ , where  $\theta(x)$  is the usual Heaviside step-function

$$\theta(x) = \begin{cases} 1 & \text{for } x > 0, \\ 0 & \text{for } x < 0. \end{cases}$$



Due to the periodic boundary conditions we have  $\Delta_1^- = \theta(x_1 - x_L)$  and  $\Delta_L^+ = \theta(x_L - x_1)$ . Using the operator formalism we can represent the expectation  $\mu_1^{1D}$  in the following form

$$\mu_1^{1D} = \int_0^1 \int_0^1 \dots \int_0^1 \left[ \sum_{i=1}^L \Delta_i^- \Delta_i^+ \right] dx_1 dx_2 \dots dx_L. \quad (27)$$

In the sum above each term  $\Delta_i^- \Delta_i^+ = \theta(x_i - x_{i-1})\theta(x_i - x_{i+1})$  corresponds to the peak at the position  $x_i$ . All  $L$  terms in the sum in (27) are identical and independent, so it is possible to rewrite (27) as

$$\mu_1^{1D} = L \int_0^1 \int_0^1 \int_0^1 \theta(x_i - x_{i-1})\theta(x_i - x_{i+1}) dx_{i-1} dx_i dx_{i+1} = L \int_0^1 \left[ \int_0^{x_i} \int_0^{x_i} dx_{i-1} dx_{i+1} \right] dx_i = \frac{1}{3}L^2. \quad (28)$$

2. The second central moment  $\mu_2^{1D}$  can be computed as follows

$$\begin{aligned} \mu_2^{1D} &\equiv \langle M^2 \rangle - \langle M \rangle^2 = \int_0^1 \int_0^1 \dots \int_0^1 \left[ \sum_{i=1}^L \sum_{j=1}^L \Delta_i^- \Delta_i^+ \Delta_j^- \Delta_j^+ \{ \delta(x_a - x_b) \} \right] dx_1 dx_2 \dots dx_L - \frac{1}{9}L^2 = \\ &= L \sum_{j=1}^L \left[ \int_0^1 \int_0^1 \int_0^1 \int_0^1 \int_0^1 \int_0^1 \Delta_i^- \Delta_i^+ \Delta_j^- \Delta_j^+ \{ \delta(x_a - x_b) \} dx_{i-1} dx_i dx_{i+1} dx_{j-1} dx_j dx_{j+1} - \frac{1}{9}L \right] \\ &= L \sum_{r=0}^3 \left[ a_r^{1D} J_r^{1D} - \frac{1}{9}L \right], \end{aligned} \quad (29)$$

where  $J_r^{1D}$  is the integral of the diagram  $r$ ,  $a_r^{1D}$  is the "weight" of the corresponding diagram (i.e. the number of identical diagrams), and the  $\delta$ -functions in eq.(29) cut off the coinciding points. For example, if in some configuration the points  $x_i$  and  $x_j$  coincide, then we include the function  $\delta(x_i - x_j)$  etc. The graphic representation of integrals in eq.(29) is given in Fig.3a. We consider the system of length  $L$  with periodic boundary conditions. Instead of summing over  $L$  possible values of  $i$  we fix some arbitrary value  $x_i$  and perform averaging over all possible positions of  $x_j$ . That gives us  $L$  in front of the sum in (29). The integral in (29) depends on  $j - i$  only. We enumerate all possible values of the integral by the index  $r$ , and compute the weight  $a_r^{1D}$  of each integral  $J_r^{1D}$  in the sum for  $j = 1, 2, \dots, L$ .

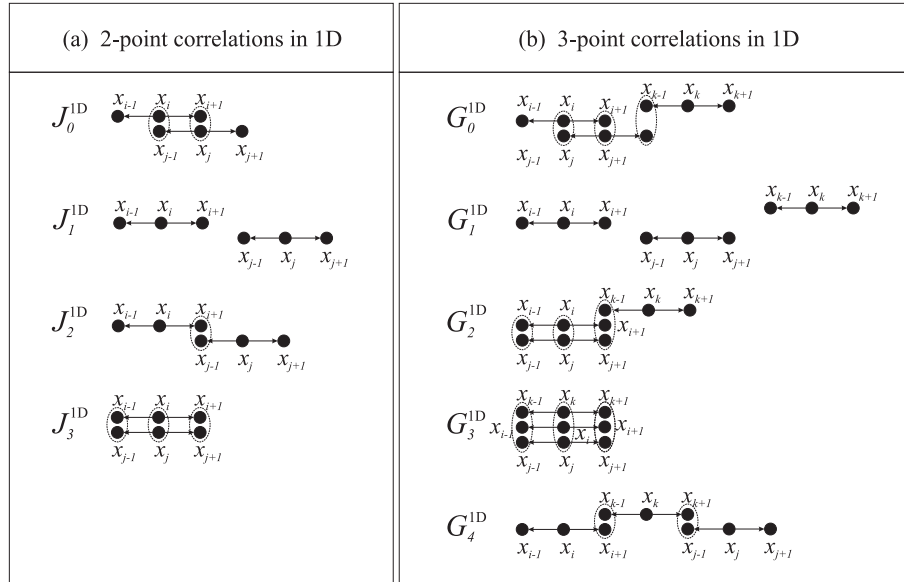


FIG. 3: Basic diagrams and corresponding integrals: a)  $J_r^{1D}$  for the computation of  $\mu_2^{1D}$ ; b)  $G_r^{1D}$  for the computation of  $\mu_3^{1D}$ .

The total number of diagrams is normalized:  $\sum_{r=0}^3 a_r^{1D} = L$ . The computed values of  $J_r^{1D}$  and of  $a_r^{1D}$  are collected in the Table I. All such configurations are generated by shifting the point  $x_j$  with respect to  $x_i$  as shown in Fig.3a,b.

integral $J_r^{1D}$	$J_0^{1D}$	$J_1^{1D}$	$J_2^{1D}$	$J_3^{1D}$
values of $J_r^{1D}$	0	$\frac{1}{9}$	$\frac{2}{15}$	$\frac{1}{3}$
weight $a_r^{1D}$	$a_0^{1D}$	$a_1^{1D}$	$a_2^{1D}$	$a_3^{1D}$
values of $a_r^{1D}$	2	$L - 5$	2	1

TABLE I: Values of diagrams  $J_r^{1D}$  and of the corresponding weights  $a_r^{1D}$  for computing  $\mu_2^{1D}$ .

If the shortest distance between  $x_i$  and  $x_j$  is larger than 2 (respecting the periodic boundary conditions), then the integrals over  $\Delta_i^- \Delta_i^+$  and  $\Delta_j^- \Delta_j^+$  decouple and give contribution  $J_1^{1D} = [P(\uparrow\downarrow)]^2 = \frac{1}{3} \times \frac{1}{3} = \frac{1}{9}$ . The contribution of these integrals cancel by subtracting  $\frac{1}{9}$ . The number of such integrals is  $a_1^{1D} = L - 5$ . The total number of all other configurations is finite and does not depend on  $L$ , so the second central moment is proportional to  $L$  but no to  $L^2$ . Substituting the values from the Table I into (29), we arrive at the following expression for the second central moment  $\mu_2^{1D}$

$$\mu_2^{1D} = L \sum_{r=0}^3 \left( a_r^{1D} J_r^{1D} - \frac{1}{9} L \right) = L \left( 2 \left( -\frac{1}{9} \right) + 2 \left( \frac{2}{15} - \frac{1}{9} \right) + \left( \frac{1}{3} - \frac{1}{9} \right) \right) = \frac{2}{45} L. \quad (30)$$

3. The computation of the third central moment  $\mu_3^{1D}$ ,

$$\mu_3^{1D} = \left\langle (M - \langle M \rangle)^3 \right\rangle = \langle M^3 \rangle - \langle M \rangle^3 - 3 \langle M \rangle \left( \langle M^2 \rangle - \langle M \rangle^2 \right), \quad (31)$$

proceeds exactly in the same way as the different lattice points. The averaged third power of  $M$  is

$$\langle M^3 \rangle = \int_0^1 \int_0^1 \dots \int_0^1 \left[ \sum_{i=1}^L \sum_{j=1}^L \sum_{k=1}^L \Delta_i^- \Delta_i^+ \Delta_j^- \Delta_j^+ \Delta_k^- \Delta_k^+ \{ \delta(x_a - x_b) \} \right] dx_1 dx_2 \dots dx_L. \quad (32)$$

This quantity depends only on integrals over three groups of points  $x_{i-1}, x_i, x_{i+1}$ ,  $x_{j-1}, x_j, x_{j+1}$  and  $x_{k-1}, x_k, x_{k+1}$  and their mutual arrangement. To proceed, we fix some position of  $x_i$  (as it has been done for  $\mu_2^{1D}$ ) and consider the positions of  $x_j$  and  $x_k$  with respect to it. Using the diagrammatic approach we compute integrals  $G_r$  in (32) for each three-point configuration. The corresponding diagrams  $G_r^{1D}$  for  $r = 0, \dots, 4$  are shown in Fig.3b. We have the following possibilities:

(i) The integral (32) contains terms like  $G_0^{1D} = \int \int \theta(x_i - x_j) \theta(x_j - x_i) dx_i dx_j = 0$ ;

(ii) All three points  $x_i, x_j, x_k$  are separate. In such a situation the integrations over three groups of points are independent, giving for each group  $\frac{1}{3}$  according to (28). So, we have  $G_1^{1D} = (P(\uparrow\downarrow))^3 = \frac{1}{27}$ . All terms of such a type in (31) cancel;

(iii) Two groups have the common points and the third group is separated from them. In this case the separated integration over the third group of points gives  $\langle M \rangle$ . The integration over the rest pair of groups gives just the same result as the contribution to the second central moment. The factor 3 in front of  $\left( \langle M^2 \rangle - \langle M \rangle^2 \right)$  corresponds to three different ways ( $ij + k$ ,  $ik + j$ ,  $jk + i$ ) to ascribe the indices to these points. Thus, the contributions from the three-points configurations of such a type and contribution of two-point configurations for  $\langle M^2 \rangle$  in (31) cancel;

(iv) At least two pairs of groups have common points. Such configurations give a non-zero contribution. Integrals for such groups  $G_r^{1D}$  and corresponding weights  $c_r^{1D}$  are summarized in the Table II where  $G_r = J_r$  for  $r = 0, 2, 3$ .

integral $G_i^{1D}$	$G_0^{1D}$	$G_1^{1D}$	$G_2^{1D}$	$G_3^{1D}$	$G_4^{1D}$	integral $J_r^{1D}$	$J_0^{1D}$	$J_1^{1D}$	$J_2^{1D}$	$J_3^{1D}$
value of $G_i^{1D}$	0	$\frac{1}{27}$	$\frac{2}{15}$	$\frac{1}{3}$	$\frac{17}{315}$	value of $J_r^{1D}$	0	$\frac{1}{9}$	$\frac{2}{15}$	$\frac{1}{3}$
weight $c_i^{1D}$	$c_0^{1D}$	$c_1^{1D}$	$c_2^{1D}$	$c_3^{1D}$	$c_4^{1D}$	weight $b_r^{1D}$	$b_0^{1D}$	$b_1^{1D}$	$b_2^{1D}$	$b_3^{1D}$
value of $c_i^{1D}$	24	$L - 37$	6	1	6	value of $b_r^{1D}$	36	18	42	15

TABLE II: Values of integrals  $G_r^{1D}$  and of the weights  $c_r^{1D}$  (left) for the three-point configurations and values of integrals  $J_r^{1D}$  and weights  $b_r^{1D}$  (right) for computing  $\mu_3^{1D}$ .

We can split nontrivial ( $r \neq 1$ ) three-point configuration ( $c_r^{1D}$ ) into the two-point configuration by deleting of the one-point group in three different ways. Thus,  $3 \sum_{\substack{r=0 \\ r \neq 1}}^4 c_r^{1D} = \sum_{q=0}^3 b_q^{1D} = 111$ , where  $b_q^{1D}$  is the number of the two-point configurations of type  $q$  obtained as a result of splitting of all possible three-points configurations. The two-point configurations  $b_r^{1D}$  are enumerated in the Table II. The contribution of the two-point configurations are not compensated by an appropriate term from the three-points configurations, so we have to take it into account manually. So, substituting expansion of (32) into (31), we obtain

$$\begin{aligned}
\mu_3^{2D} &= \langle M^3 \rangle - \langle M \rangle^3 - 3 \langle M \rangle (\langle M^2 \rangle - \langle M \rangle^2) = \\
&= L \left[ \sum_{r=0}^4 \left( c_r G_r^{1D} - \frac{1}{27} L \right) - \frac{1}{3} \sum_{q=0}^3 b_q \left( J_q - \frac{1}{9} \right) \right] \\
&= L \left[ 6 \frac{2}{15} + 6 \frac{17}{315} + \frac{1}{3} - 37 \frac{1}{27} - \frac{1}{3} \left( 36 \times 0 + 18 \frac{1}{9} + 42 \frac{2}{15} + 15 \frac{1}{3} \right) + 111 \frac{1}{27} \right] \\
&= -\frac{2}{945} L \simeq -0.0021164L.
\end{aligned} \tag{33}$$

It is worth mentioning that the moments in Eqs.(28), (30) and (33), calculated using the operator technique, coincide with the ones obtained on the basis of exact combinatorial approach (16).

### E. Probability $p(l)$ of two peaks separated by distance $l$

We aim now at evaluating the conditional probability  $p(l)$  of having two peaks separated by a distance  $l$ , under the condition that there are no peaks (i.e. sequences  $\uparrow \downarrow$ ) on the interval between these peaks. According to [22], this probability is given by

$$p(l) = \int_0^1 dx \sum Q(x), \tag{34}$$

where the sum is taken over all possible peak-avoiding rise-and-descent patterns of length  $l$  inbetween of two peaks, while  $Q(x)$  denote the  $Q$ -polynomials corresponding to each given configuration (see the explanations above).

There are several possible peak-avoiding "rise-and-descent" sequences contributing to such a probability. These sequences are depicted in Fig.4. The first peak is located at 0 position, the second peak is located at  $l$  position. We have fix descent at 1st position (variable  $Y$ ) to keep a peak at the 0s position (variable  $X$ ).

Now, the  $Q$ -polynomial associated with the sequence (a) in Fig.4 has the following form:

$$Q^a(x) = \int_x^1 dX \int_0^X dY \int_Y^1 dx_1 \int_{x_1}^1 dx_2 \dots \int_{x_{l-2}}^1 dx_{l-1} \int_0^{x_{l-1}} dx_l. \tag{35}$$

Performing the integration over  $x_{l+1}$  in the latter expression, we denote the multiple integrals over the variables  $x_k$ ,  $k = 1, 2, 3 \dots, l$  as

$$M_l(Y) = \int_Y^1 dx_1 \int_{x_1}^1 dx_2 \dots \int_{x_{l-1}}^1 x_l dx_l. \tag{36}$$

Notice now that  $M_l$  obey the following recursion scheme:

$$M_l(Y) = \int_Y^1 M_{l-1}(X) dX, \quad M_0(Y) = Y. \tag{37}$$

Introducing the generating function of the form:

$$M(Y) = \sum_{l=0}^{\infty} M_l(Y) z^l, \tag{38}$$

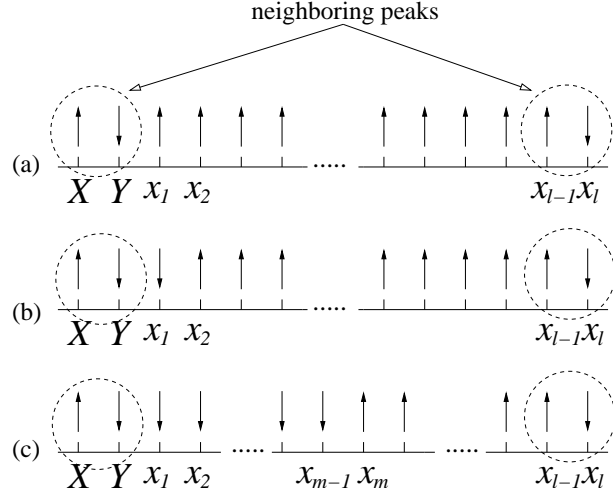


FIG. 4: Rise-and-descent patterns contributing to the conditional probability of having two closest peaks at distance  $l$  apart from each other. Configuration (a) has only one descent inbetween of two peaks. Configuration (b) has a two descents following the first peak and (c) presents a generalization of (b) over configurations having  $m$  descents, ( $m = 1, 2, \dots, l$ ), after the first peak which are followed by  $l - m$  rises.

we readily find that it obeys

$$M(Y) - Y = z \int_Y^1 M(X) dX, \quad (39)$$

and consequently,  $M_l$  are simply the coefficients in the expansion

$$M(Y) = \sum_{l=0}^{\infty} M_l z^l = \frac{1}{z} \left[ 1 - (1-z) \exp(z(1-x)) \right], \quad (40)$$

which are given explicitly by

$$M_l(Y) = \frac{(1-Y)^l}{l!} - \frac{(1-Y)^{l+1}}{(l+1)!} = \frac{1}{(l+1)!} (l+Y)(1-Y)^l. \quad (41)$$

Hence, the  $Q$ -polynomial associated with the configuration (a) in Fig.4 obeys

$$Q^a(x) = \int_x^1 dX \int_0^X M_{l-1}(Y) dY = \frac{1}{l!} \int_x^1 dX \int_0^X [(1-Y)^{l-1} (l-1+Y)] dY, \quad (42)$$

and the contribution of this very configuration to the probability  $p(l)$  reads:

$$p^a(l) = \frac{1}{l!} \int_0^1 dx \int_x^1 dX \int_0^X [(1-Y)^{l-1} (l-1+Y)] dY. \quad (43)$$

Next, we turn to the contribution coming out of the general configuration (c) in Fig.4. The  $Q$ -polynomial associated with this configuration of rises and descents for a fixed  $m$  is given by

$$\begin{aligned} Q^c(x, m) &= \int_x^1 dX \int_0^X dY \int_0^Y dx_1 \int_0^{x_1} dx_2 \int_0^{x_2} dx_3 \dots \int_0^{x_{m-2}} dx_{m-1} \int_{x_{m-1}}^1 dx_m \dots \int_{x_{l-2}}^1 dx_{l-1} \int_0^{x_{l-1}} dx_l \\ &= \int_x^1 dX \int_0^X dY \int_0^Y dx_1 \int_0^{x_1} dx_2 \int_0^{x_2} dx_3 \dots \int_0^{x_{m-2}} dx_{m-1} \int_{x_{m-1}}^1 dx_m \dots \int_{x_{l-2}}^1 dx_{l-1} dx_l \\ &= \int_x^1 dX \int_0^X dY \int_0^Y dx_1 \int_0^{x_1} dx_2 \int_0^{x_2} dx_3 \dots \int_0^{x_{m-2}} M_{l-m}(x_{m-1}) dx_{m-1}. \end{aligned} \quad (44)$$

Let us note, that  $Q^a(x) = Q^c(x, m = 1)$ . Consider next a recursion scheme of the form

$$N_m(Y) = z \int_0^Y N_{m-1}(X) dX, \quad (45)$$

where  $N_0(Y)$  is some arbitrary function  $\Phi(Y)$ . Introducing the generating function

$$N(Y) = \sum_{m=0}^{\infty} N_m(Y) z^m, \quad (46)$$

we get that it obeys

$$N(Y) - \Phi(Y) = z \int_0^Y N(X) dX. \quad (47)$$

Solution of the latter equation can be readily obtained by standard means and reads

$$N(Y) = \Phi(0) \exp(zY) + \int_0^Y \frac{d\Phi(X)}{dX} \exp(z(Y-X)) dX. \quad (48)$$

Finally, expanding the rhs of the latter equation in powers of  $z$ , we get that  $N_m(Y)$  are given explicitly by

$$N_m(Y) = \Phi(0) \frac{Y^m}{m!} + \int_0^Y \frac{d\Phi(X)}{dX} \frac{(Y-X)^m}{m!} dX = \int_0^Y \Phi(X) \frac{(Y-X)^{m-1}}{(m-1)!} dX. \quad (49)$$

Now, we notice that, as a matter of fact, the multiple integral over the variables  $Y$  and  $x_k, k = 1, 2, \dots, m-1$  on the rhs of Eq.(44) becomes just the function  $N_m(Y)$ , if one takes  $\Phi(Y) = M_{l-m}(Y)$ . This implies that

$$\int_0^X dY \int_0^Y dx_1 \int_0^{x_1} dx_2 \dots \int_0^{x_{m-2}} M_{l-m}(x_{m-1}) dx_{m-1} = \int_0^X \frac{(X-Y)^{m-1} (1-Y)^{l-m} (l-m+Y)}{(m-1)! (l-m+1)!} dY. \quad (50)$$

Substituting  $m = 1$  we obtain here  $\int_0^X M_{l-1} dY$ . Consequently, we find that the desired probability obeys

$$p(l) = \int_0^1 dx \int_x^1 dX \int_0^X \left[ \sum_{m=1}^{l-1} \frac{(X-Y)^{m-1} (1-Y)^{l-m} (l-m+Y)}{(m-1)! (l-m+1)!} \right] dY. \quad (51)$$

Let us introduce the generating function  $F(z) = \sum_{l=2}^{\infty} z^l p(l)$ . We can represent the sum

$$\sum_{l=2}^{\infty} \sum_{m=1}^{l-1} z^l f(l, m) = \sum_{m=1}^{\infty} \sum_{k=1}^{\infty} z^{k+m} f(k+m, m), \quad (52)$$

where  $k = l - m$ . Using

$$\sum_{m=1}^{\infty} z^m \frac{(X-Y)^{m-1}}{(m-1)!} = z e^{z(X-Y)}, \quad (53)$$

and

$$\sum_{k=1}^{\infty} z^k (k+Y) \frac{(1-Y)^k}{(k+1)!} = e^{z(1-Y)} \left( 1 - \frac{1}{z} \right) + \frac{1}{z} - Y, \quad (54)$$

we obtain

$$\begin{aligned}
F(z) &= \sum_{l=2}^{\infty} z^l \left( \int_0^1 dx \int_x^1 dX \int_0^X \left[ \sum_{m=1}^{l-1} \frac{(X-Y)^{m-1} (1-Y)^{l-m} (l-m+Y)}{(m-1)!(l-m+1)!} \right] dY \right) \\
&= \int_0^1 dx \int_x^1 dX \int_0^X \left[ \sum_{m=1}^{\infty} \sum_{k=1}^{\infty} \left( z^m \frac{(X-Y)^{m-1}}{(m-1)!} \right) \left( z^k \frac{(1-Y)^k (k+Y)}{(k+1)!} \right) \right] dY \\
&= \int_0^1 dx \int_x^1 dX \int_0^X \left[ z e^{z(X-Y)} \left( e^{z(1-Y)} \left( 1 - \frac{1}{z} \right) - Y + \frac{1}{z} \right) \right] dY \\
&= \frac{(z-1)^2}{2z^3} e^{2z} + \left( \frac{1}{3} + \frac{1}{2z} - \frac{1}{2z^3} \right).
\end{aligned} \tag{55}$$

Hence, the generating function is given by

$$F(z) = \frac{2}{15} z^2 + \frac{1}{9} z^3 + \frac{2}{35} z^4 + \frac{1}{45} z^5 + \frac{4}{567} z^6 + \dots \tag{56}$$

Note that the numerical values  $\frac{2}{15}$  (for  $l=2$ ) and  $\frac{1}{9}$  (for  $l=3$ ) correspond to the values obtained in [22]. In general, we get the following explicit expression

$$p(l) = \frac{1}{2} \left( \frac{2^{l+1}}{(l+1)!} - 2 \frac{2^{l+2}}{(l+2)!} + \frac{2^{l+3}}{(l+3)!} \right) = 2^l \frac{(l-1)(l+2)}{(l+3)!}, \tag{57}$$

which defines the probability  $p(l)$  of finding two peaks separated by the distance  $l$  with no peaks inbetween these two points for arbitrary  $l$ .

### III. TWO-DIMENSIONAL BALLISTIC DEPOSITION

#### A. Basic definitions

The process of a two-dimensional ballistic deposition in a box with a square base  $L \times L$  can be viewed as a sequential adding of elementary cubes in the columns satisfying the following rules (compare to (1)):

$$h(i, j, n+1) = \max\{h(i-1, j, n), h(i+1, j, n), h(i, j, n), h(i, j-1, n), h(i, j+1, n)\} + 1, \tag{58}$$

where  $h(i, j, n)$  is the height of the column with coordinates  $(i, j)$  ( $1 \leq \{i, j\} \leq L$ ) at deposition moment  $n$  ( $1 \leq n \leq N$ ). The cubes are added to the columns with the uniform distribution – see Fig.5. The “peak” of a two-dimensional landscape  $h(i, j, n)$  is defined as a local maximum in the set  $\{h(i, j, n)\}$  for some fixed moment  $n$ :

$$\begin{cases} h(i, j, n) > h(i-1, j, n) \\ h(i, j, n) > h(i+1, j, n) \\ h(i, j, n) > h(i, j-1, n) \\ h(i, j, n) > h(i, j+1, n) \end{cases} \tag{59}$$

Let us note that (58)–(59) imply the periodic boundary conditions both in  $i$  and  $j$  coordinates ( $1 \leq \{i, j\} \leq L$ ). The influence of boundary condition on the expectation, variance and higher moments of peak numbers can be easily estimated and becomes negligible in the limit  $L \rightarrow \infty$ .

In what follows we are going to study the statistics of peaks in a two-dimensional landscape  $h(i, j, n)$  by converting this problem to the search of the distribution of peaks in the associated permutation matrix. However the definition of a “peak” in the corresponding permutation matrix should be modified in order to take into account the two-dimensional nature of the ballistic aggregation.

It is convenient to represent the two-dimensional base  $(i, j)$  as a one-dimensional set with long-ranged correlations. Namely, reading the lattice  $(i, j)$  from left to right in the line and line-by-line from top-to-bottom, as an electron

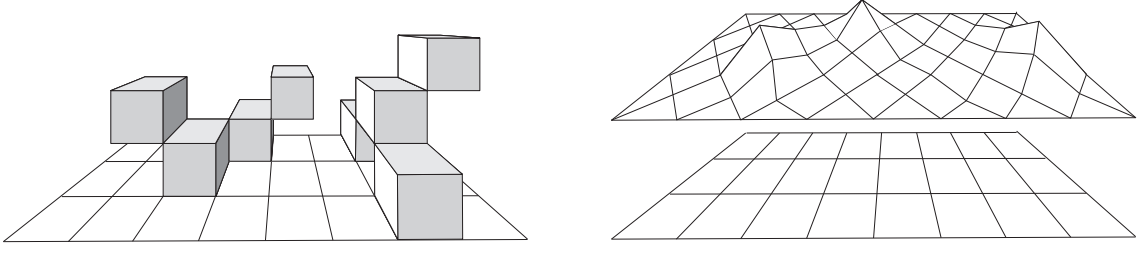


FIG. 5: The two-dimensional ballistic deposition and the corresponding random landscape.

beam does to highlight the image on the TV screen, we can rewrite the equations (58) and (59) using the redefinition:  $h(i, j, n) \equiv h(k, n)$ . Hence,  $h(i-1, j, n) \equiv h(k-1, n)$ ;  $h(i+1, j, n) \equiv h(k+1, n)$ ;  $h(i, j-1, n) \equiv h(k-L, n)$ ;  $h(i, j+1, n) \equiv h(k+L, n)$ , where  $1 \leq k \leq L^2$ .

Given Eq.(58), we can describe the growth of a two-dimensional landscape over the base  $L \times L$  as a stationary “updating dynamics” in the  $L^2 \times L^2$  permutation matrix with the uniform distribution on updating events. The uniform “updating dynamics” on permutations generates the PDF of peaks identical to the PDF of peaks computed over the ensemble of all  $(L^2)!$  equally weighted permutations (compare to the one-dimensional case). Thus, repeating the arguments of the previous section, we can construct the PGRW<sup>2D</sup> for permutation matrix with finite-length correlations. The main difference between one- and two-dimensional models deals with the definition of a peak. In the 1D case the peak appears in the position  $k$  of the permutation matrix if the corresponding permutation  $\pi_k$  is larger than the nearest neighboring permutations  $\pi_{k-1}, \pi_{k+1}$ . In the 2D case the permutation is a peak if and only if  $\pi_k$  is larger than  $\pi_{k-1}, \pi_{k+1}, \pi_{k-L}, \pi_{k+L}$ . In the next Section we generalize the operator formalism to the 2D case and compute the PDF of peaks for the 2D uniform BD process.

### B. Moments of the probability distribution function in 2D

To obtain the limiting Probability Distribution Function  $P(M, N)$  of having exactly  $M$  peaks of a two-dimensional landscape obtained by the ballistic deposition above the square base  $N = L \times L$  ( $L \rightarrow \infty$ ), we calculate the first three central moments of the distribution function and then compare them with the first terms of the Edgeworth series [23]. This enables us: a) to show that in the limit  $L \rightarrow \infty$  the function  $P(M, N)$  converges to the Gaussian distribution, and b) to present an explicit expression for  $P(M, N)$  in this limit.

The total number of points for 2D system is  $N = L^2$ . Applying to the 2D case the same arguments as in 1D case, we can define

$$\begin{aligned}
 \Delta_{i,j}^{\uparrow} &= \theta(x_{i,j} - x_{i-1,j}) \text{ for up neighbor} \\
 \Delta_{i,j}^{\rightarrow} &= \theta(x_{i,j} - x_{i,j+1}) \text{ for right neighbor} \\
 \Delta_{i,j}^{\downarrow} &= \theta(x_{i,j} - x_{i+1,j}) \text{ for down neighbor} \\
 \Delta_{i,j}^{\leftarrow} &= \theta(x_{i,j} - x_{i,j-1}) \text{ for left neighbor,}
 \end{aligned} \tag{60}$$

(compare (60) to (26)).

1. Using the operator formalism we obtain for the first moment

$$\begin{aligned}
 \mu_1^{2D} &= \int_0^1 \dots \int_0^1 \left[ \sum_{i=1}^L \sum_{j=1}^L \Delta_{i,j}^{\uparrow} \Delta_{i,j}^{\rightarrow} \Delta_{i,j}^{\downarrow} \Delta_{i,j}^{\leftarrow} \right] dx_{1,1} dx_{1,2} \dots dx_{L,L-1} dx_{L,L} \\
 &= N \int_0^1 \int_0^1 \int_0^1 \int_0^1 \int_0^1 \Delta_{i,j}^{\uparrow} \Delta_{i,j}^{\rightarrow} \Delta_{i,j}^{\downarrow} \Delta_{i,j}^{\leftarrow} dx_{i-1,j} dx_{i,j+1} dx_{i+1,j} dx_{i,j-1} dx_{i,j} = \frac{1}{5} N.
 \end{aligned} \tag{61}$$

As in 1D, all terms in (61) are identical and independent.

2. The same method is used for computing the second central moment. We define  $dx_{i,j} = dx_{i-1,j}dx_{i,j+1}dx_{i+1,j}dx_{i,j-1}dx_{i,j}$  for integration over the point  $x_{i,j}$  and its four neighbors to make the expressions more compact. Instead of summing over  $i, j$ , we fix the position of the first point  $x_{i,j}$  and perform the summation over all possible positions of  $x_{k,l}$  with respect to  $x_{i,j}$ . Then we enumerate all different integrals  $J_r^{2D}$  and compute the corresponding weights  $a_r^{2D}$ . The configurations which contribute to  $J_r^{2D}$  are shown in Fig.6a,b. As in 1D case the  $\delta$ -functions  $\delta(x_{a,b} - x_{c,d})$  cut off the coinciding points.

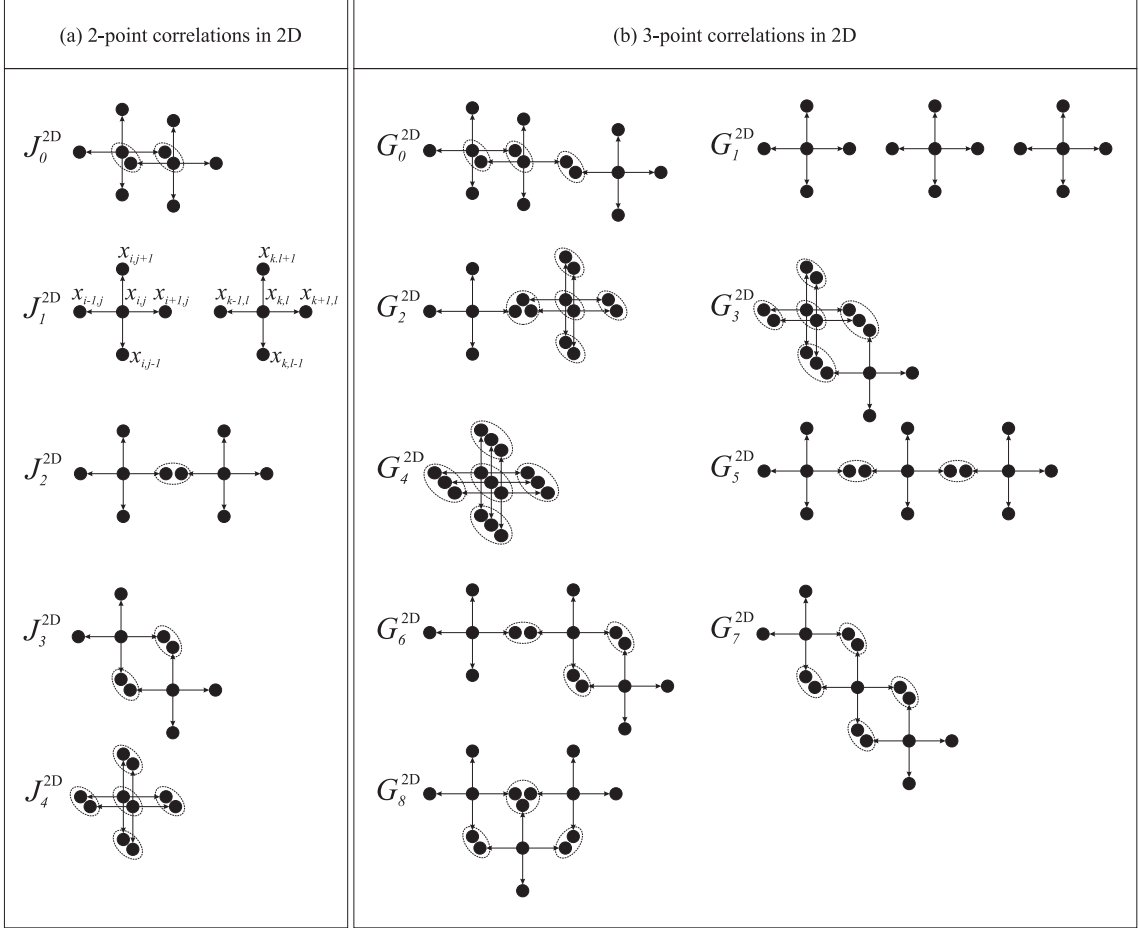


FIG. 6: Basic diagrams and corresponding integrals: a)  $J_r^{2D}$  for the computation of  $\mu_2^{2D}$ ; b)  $G_r^{2D}$  for the computation of  $\mu_3^{2D}$ .

The values of integrals  $J_r^{2D}$  and their weights  $a_r^{2D}$  are collected in Table III.

integral $J_r^{2D}$	$J_0^{2D}$	$J_1^{2D}$	$J_2^{2D}$	$J_3^{2D}$	$J_4^{2D}$
value of $J_r^{2D}$	0	$\frac{1}{25}$	$\frac{2}{45}$	$\frac{1}{20}$	$\frac{1}{5}$
weight $a_r^{2D}$	$a_0^{2D}$	$a_1^{2D}$	$a_2^{2D}$	$a_3^{2D}$	$a_4^{2D}$
value of $a_r^{2D}$	4	$N - 13$	4	4	1

TABLE III: Values of integrals  $J_r^{2D}$  and of the weights  $a_r^{2D}$  for computing  $\mu_2^{2D}$ .

The total number of integrals is  $\sum_{r=0}^4 a_r^{2D} = N = L^2$ . The contribution from the integral  $J_1^{2D}$  is exactly cancelled by



the term  $-\frac{1}{25}$  coming from two independent points:

$$\begin{aligned}
\mu_2^{2D} &= \int_0^1 \dots \int_0^1 \left[ \sum_{i=1}^L \sum_{j=1}^L \sum_{k=1}^L \sum_{l=1}^L \Delta_{i,j}^\uparrow \Delta_{i,j}^\rightarrow \Delta_{i,j}^\downarrow \Delta_{i,j}^\leftarrow \Delta_{k,l}^\uparrow \Delta_{k,l}^\rightarrow \Delta_{k,l}^\downarrow \Delta_{k,l}^\leftarrow \{\delta(x_{a,b} - x_{c,d})\} \right] dx_{1,1} dx_{2,1} \dots dx_{L,L} - \frac{1}{25} N^2 \\
&= N \sum_{k=1}^L \sum_{l=1}^L \left[ \int_0^1 \dots \int_0^1 \Delta_{i,j}^\uparrow \Delta_{i,j}^\rightarrow \Delta_{i,j}^\downarrow \Delta_{i,j}^\leftarrow \Delta_{k,l}^\uparrow \Delta_{k,l}^\rightarrow \Delta_{k,l}^\downarrow \Delta_{k,l}^\leftarrow \{\delta(x_{a,b} - x_{c,d})\} d\mathbf{x}_{i,j} d\mathbf{x}_{k,l} - \frac{1}{25} N \right] \\
&= N \sum_{r=0}^4 \left[ a_r^{2D} J_r^{2D} - \frac{1}{25} N \right] = \left( 4 \times \frac{1}{20} + 4 \times \frac{2}{45} + \frac{1}{5} - 13 \times \frac{1}{25} \right) N = \frac{13}{225} N.
\end{aligned} \tag{62}$$

3. For computation of the third moment in 2D we use again the same method as in 1D. Namely, we fix the first point  $x_{i,j}$  and enumerate all possible configurations of three points. Different types of three-points configurations are depicted in Fig.6b). Other configurations with the same contribution  $G_r^{2D}$  and the same topologies but slightly different conformations are not shown in the figure. The integrals  $G_r^{2D}$  and  $J_r^{2D}$  have the same values for  $r = 0, 2, 3, 4$ . In the configuration  $G_4^{2D}$  all three points coincide, so  $G_4^{2D} = \frac{1}{5}$ . The most general form of the integral  $G_r^{2D}$  is as follows

$$G_r^{2D} = \int_0^1 \dots \int_0^1 \Delta_{i,j}^\uparrow \Delta_{i,j}^\rightarrow \Delta_{i,j}^\downarrow \Delta_{i,j}^\leftarrow \Delta_{k,l}^\uparrow \Delta_{k,l}^\rightarrow \Delta_{k,l}^\downarrow \Delta_{k,l}^\leftarrow \Delta_{m,n}^\uparrow \Delta_{m,n}^\rightarrow \Delta_{m,n}^\downarrow \Delta_{m,n}^\leftarrow \{\delta(x_{a,b} - x_{c,d})\} d\mathbf{x}_{i,j} d\mathbf{x}_{k,l} d\mathbf{x}_{m,n}, \tag{63}$$

where  $d\mathbf{x}_{i,j} = dx_{i-1,j} dx_{i,j-1} dx_{i+1,j} dx_{i,j+1} dx_{i,j}$  and the  $\delta$ -functions in (63) cut off the coinciding points. For example, if in some configuration the points  $x_{i,j+1}$  and  $x_{k,l-1}$  coincide, then we include the function  $\delta(x_{k,l-1} - x_{i,j+1})$  etc.

It is possible to simplify integrals of such a type by changing the limits of integration. For example,  $\int_0^1 \int_0^1 \Delta_{i,j}^\uparrow dx_{i,j} dx_{i-1,j} = \int_0^1 x_{i,j} dx_{i,j}$ . In such a way the integral  $G_5^{2D}$  can be expressed as follows:

$$G_5^{2D} = \int_0^1 dx_{i,j} \left[ x_{i,j}^3 \int_0^{x_{i,j}} dx_{i,j+1} \left[ \int_{dx_{i,j+1}}^1 dx_{i,j+2} \left[ x_{i,j+2}^2 \int_0^{x_{i,j+2}} dx_{i,j+3} \left[ \int_{dx_{i,j+4}}^1 x_{i,j+4}^3 dx_{i,j+4} \right] \right] \right] \right] \right] = \frac{29}{2925}. \tag{64}$$

The values of integrals  $G_0^{2D} - G_8^{2D}$  are collected in the Table IV.

integral $G_r^{2D}$	$G_0^{2D}$	$G_1^{2D}$	$G_2^{2D}$	$G_3^{2D}$	$G_4^{2D}$	$G_5^{2D}$	$G_6^{2D}$	$G_7^{2D}$	$G_8^{2D}$	integral $J_r^{2D}$	$J_0^{2D}$	$J_1^{2D}$	$J_2^{2D}$	$J_3^{2D}$	$J_4^{2D}$
value	0	$\frac{1}{125}$	$\frac{2}{45}$	$\frac{1}{20}$	$\frac{1}{5}$	$\frac{29}{2925}$	$\frac{121}{10800}$	$\frac{7}{550}$	$\frac{13}{990}$	value of $J_r^{2D}$	0	$\frac{1}{25}$	$\frac{2}{45}$	$\frac{1}{20}$	$\frac{1}{5}$
weight $c_r^{2D}$	$c_0^{2D}$	$c_1^{2D}$	$c_2^{2D}$	$c_3^{2D}$	$c_4^{2D}$	$c_5^{2D}$	$c_6^{2D}$	$c_7^{2D}$	$c_8^{2D}$	weight $b_r^{2D}$	$b_0^{2D}$	$b_1^{2D}$	$b_2^{2D}$	$b_3^{2D}$	$b_4^{2D}$
value of $c_r^{2D}$	168	$N - 313$	12	12	1	36	48	12	24	value of $b_r^{2D}$	216	216	252	216	39

TABLE IV: The three-point configurations for computing  $\mu_3^{2D}$ : integrals  $G_r^{2D}$  and weights  $c_r^{2D}$  (left) and integrals  $J_r^{2D}$  and weights  $b_r^{2D}$  (right).

The symmetry of configurations defines the weights  $c_r$ . For example, the diagram of the integral  $G_5^{2D}$  in Fig.6b has two orientations along vertical and horizontal lines. Thus the total weight of the integral  $G_5^{2D}$  is  $c_5^{2D} = 36$ .

The values of  $c_r$  are given in the Table IV. Totally there are  $\sum_{\substack{r=0 \\ r \neq 1}}^8 c_r^{2D} = 313$  different nontrivial configurations. We can split each of the nontrivial three-points configuration as it has been done in 1D case. There are three ways to do it. Values of  $b_r$  of the corresponding two-point configurations are shown in the Table IV with the total number

$\sum_{r=0}^4 b_r^{2D} = 939$  of such configurations. Now it is possible to compute the third moment

$$\begin{aligned} \mu_3^{2D} &= N \left[ \sum_{r=0}^8 \left( c_r^{2D} G_r^{2D} - \frac{1}{125} N \right) - \frac{1}{5} \sum_{r=0}^4 b_r^{2D} \left( J_r^{2D} - \frac{1}{25} \right) \right] \\ &= N \left[ 12 \frac{2}{45} + 12 \frac{1}{20} + 36 \frac{29}{2925} + 48 \frac{121}{10800} + 12 \frac{7}{550} + 24 \frac{13}{990} + \frac{1}{5} - 313 \frac{1}{125} - \right. \\ &\quad \left. - \frac{1}{5} \left( 216 \frac{1}{25} + 252 \frac{2}{45} + 216 \frac{1}{20} + 39 \frac{1}{5} \right) + 939 \frac{1}{125} \right] = \frac{512}{32175} N \simeq 0.015913N. \end{aligned} \quad (65)$$

### C. The distribution function $P(M, L)$ in the scaling limit

The second and the third cumulants of  $P(M, N)$  in 2D are equal the second and the third central moments:

$$\begin{cases} \kappa_2^{2D} = \mu_2^{2D} = \sigma^2 = \frac{13}{225} N \\ \kappa_3^{2D} = \mu_3^{2D} = \frac{512}{32175} N \end{cases} \quad (66)$$

Introducing the normalized deviation,  $x = \frac{M - \mu_1^{2D}}{\sigma}$ , we can write the normalized probability distribution  $p(x, N) = P(\mu_1^{2D} + x\sigma, N)$  in a form of the Edgeworth series (cumulant expansion) [23]

$$p(x, N) \simeq g(x) \left( 1 + \frac{1}{\sqrt{N}} f(x) + o\left(\frac{1}{\sqrt{N}}\right) \right), \quad (67)$$

where  $g(x)$  is the Gaussian function  $g(x) = \frac{1}{\sqrt{2\pi}} e^{-x^2/2}$ , and  $f(x)$  is defined by  $\mu_2^{2D}$  and  $\mu_3^{2D}$  (see [23] for details)

$$f(x) = \sqrt{N} \frac{\kappa_3^{2D}}{(\kappa_2^{2D})^{3/2}} \frac{1}{6} (x^3 - 3x) \quad (68)$$

Substituting (66) in (68), we get

$$f(x) = \frac{512}{32175} \left( \frac{225}{13} \right)^{3/2} \frac{1}{6} (x^3 - 3x). \quad (69)$$

Let us point out that the function  $f(x)$  does not depend on  $N$ . In order to validate (69) we have performed the numerical simulations for the discrete 2D permutation-generated model with the periodic boundary conditions and have computed the distribution function  $p(x, N)$  numerically. In Fig.7a the data of the numerical simulations for  $p(x, N)$  is plotted in comparison with the Gaussian function  $g(x)$  for a system sizes  $N = 100, 256$ , while in Fig.7b the deviation of the numerically computed function  $p(x, N)$  from the Gaussian function  $g(x)$  is analyzed for  $N = 100, 256$  by plotting the fraction  $\frac{p(x, N)}{g(x)}$  with respect to the first term of the Edgeworth series  $1 + \frac{1}{\sqrt{N}} f(x)$ .

We clearly see that for  $N \rightarrow \infty$  the normalized probability distribution function  $p(x, N)$  tends to the Gaussian function  $g(x)$ .

## IV. CONCLUSION

In this work we have analysed the form of the Probability Distribution Functions of the number of local maxima (“peaks”) in one- and two-dimensional models of uniform ballistic growth. Our approach was based on two important observations: i) uniform ballistic growth process in the steady state can be considered as the statistics of equally

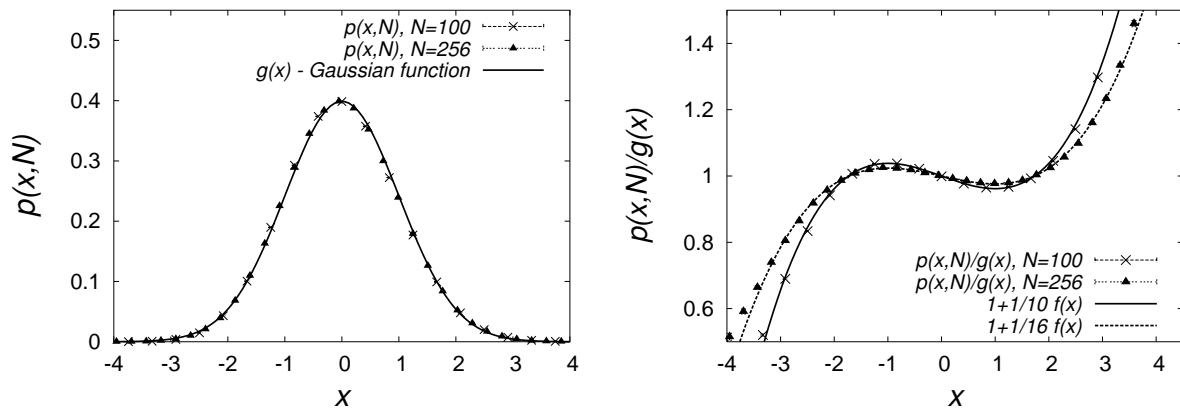


FIG. 7: (a) The results of numerical simulation of  $p(x, N)$  for  $N = 100, 256$ : (a) the comparison of  $p(x, N)$  with the Gaussian function  $g(x)$ ; (b) the comparison of the function  $p(x, N)/g(x)$  with  $1 + \frac{1}{\sqrt{N}}f(x)$ .

weighted permutations, and ii) the statistics of permutations can be efficiently treated in the framework of the operator formalism developed for the "permutation-generated random walk" [22].

In one-dimensional case the full distribution function  $P(M, L)$  of having  $M$  peaks in a bounding box of size  $L$  in a steady state, has been obtained from the expression (18) by Fourier and inverse Laplace transforms.

Besides, the operator formalism allowed us to calculate the correlation function  $p(l)$ , defining the conditional probability of having two peaks separated by a distance  $l$ , under the condition that there are no peaks in the interval between these peaks. The function  $p(l)$  is given by expression (57).

The probability distribution function of the number of local maxima in the two-dimensional case has been obtained by generalizing the concept of the permutation matrix and by considering the equally weighted ensemble of permutation matrices with properly introduced long-ranged correlations. Extending the operator formalism of [22] to the correlated permutations, we have computed three first central moments of the requested PDF. Knowing these moments, we have restored the function  $P(M, N)$  in the scaling limit  $L \rightarrow \infty$  using expansions in the Edgeworth series [23]—see (67)–(69).

### Acknowledgments

The authors are grateful to Raphael Voituriez for numerous helpful discussions of the problem. F.H. and S.N. discussed many aspects of this work during the stay in the laboratory LIFR–MIIP (Moscow), they want to thank the members of this laboratory for hearty welcome; G.O. acknowledges financial support from the Alexander von Humboldt Foundation via the Bessel Research Award. The work is partially supported by the grant ACI-NIM-2004-243 "Nouvelles Interfaces des Mathématiques" (France).

- 
- [1] L. Niemeyer, L. Pietronero, H.J. Wiessmann, Phys. Rev. Lett. **52**, 1033 (1984); M. B. Hastings, J. Stat. Phys., **107**, 1031 (2002)
- [2] M. Kadar, G. Parisi, Y. Zhang, Phys. Rev. Lett. **56**, 889 (1986)
- [3] S.F. Edwards, D.R. Wilkinson, Proc. Roy. Soc. London A **381**, 17 (1982)
- [4] S.N. Majumdar, A. Comtet, Phys. Rev. Lett. **92**, 225501 (2004)
- [5] M.A. Herman, H. Sitter, *Molecular Beam Epitaxy: Fundamentals and Current*, (Springer: Berlin, 1996)
- [6] P. Meakin, *Fractals, Scaling, and Growth Far From Equilibrium*, (Cambridge University Press: Cambridge, 1998)
- [7] M. Prähofer, H. Spohn, Phys. Rev. Lett. **84**, 4882 (2000)
- [8] J. Baik, E.M. Rains, J. Stat. Phys., **100**, 523 (2000)
- [9] K. Johansson, Comm. Math. Phys. **242**, 277 (2003)
- [10] C.A. Tracy, H. Widom, Commun. Math. Phys. **159**, 151 (1994)

- [11] B.B. Mandelbrot, *The Fractal Geometry of Nature*, (Freeman, New York, 1982)
- [12] P. Meakin, P. Ramanlal, L. M. Sander, R. C. Ball, Phys. Rev. A **34**, 5091 (1986)
- [13] J. Krug, P. Meakin, Phys. Rev. A **40**, 2064 (1989)
- [14] D. Blomker, S. Maier-Paape, T. Wanner, Interfaces and Free Boundaries, **3**, 465 (2001)
- [15] G. Costanza, Phys. Rev. E **55**, 6501 (1997); F.D.A. Aarao Reis, Phys. Rev. E **63**, 056116 (2001)
- [16] S. Nechaev, R. Bikbov, Phys. Rev. Lett. **87**, 150602 (2001)
- [17] Z. Toroczkai, G. Korniss, S. Das Sarma, R. K. P. Zia, Phys. Rev. E **62**, 276 (2000)
- [18] J. Desbois, J. Phys. A: Math. Gen. **34**, 1953 (2001)
- [19] J.R. Stembridge, Trans. Am. Math. Soc. **349**, 763 (1997)
- [20] N. Bergeron, F. Hivert, J.-Y. Thibon, J. Combinatorial Theory A, **117**, 1 (2004)
- [21] L.J. Billera, S.K.Hsiao, S. Van Willigenburg, Adv. Math. **176**, 248 (2003)
- [22] G. Oshanin, R. Voiturie, J. Phys. A: Math. Gen. **37**, 6221 (2004)
- [23] H. Cramér, *Mathematical Methods of Statistics*, (Princeton University Press: Princeton, 1957)
- [24] Only the particle of the roof  $\mathcal{T}$  can be removed from the pile without disturbing the rest of the heap—as in the *micado* game.